Journal of Visualization, Vol. 10, No. 1 (2007)39-46

Visualization of Saltating Sand Particle Movement near a Flat Ground Surface

Zhang, W.*, Kang, J. H.* and Lee, S. J.*

*1 Dept. of Mechanical Engineering, Pohang University of Science and Technology, Pohang 790-784, Korea. E-mail: sjlee@postech.ac.kr

Received 3 June 2006
Revised 25 July 2006

Abstract : Movement of natural sand particles (d = 200 - 300 μm) in a simulated atmospheric boundary layer was visualized using a digital high-speed camera. The consecutive particle images recorded at 2000 fps (frame per second) enabled us to observe the particle transport in detail, especially near the flat sand surface. Various modes of sand saltation were identified. The transverse motion of particles, often ignored in previous studies, was also visualized. In addition, instantaneous velocity fields of saltating particles were obtained using a particle tracking velocimetry (PTV), and statistical analysis of saltating particle trajectories was performed. The qualitative and quantitative results of the present study will be useful for understanding the basic physics of transport of saltating sand particles.

Keywords : Visualization, High-speed photography, Saltation, PTV, sand particles.

1. Introduction

The transport of wind-blown sand has received considerable attention. In particular, trajectories of saltating sand particles are of great interest because they are closely related with the particle concentration, the streamwise mass flux, the momentum flux and the energy flux.

Trajectories of saltating sand have been investigated by means of cinematic or high-speed photography. Bagnold (1954) found that most particles ejected vertically into the air at the initial stage of each jump, facilitating a basic assumption that the initial ejection angle is 90°. Willett and Rice (1985) used a high-speed camera to visualize the collisions of the saltating sand particles on a sand bed surface. Nalpanis et al. (1993) employed a multiple-image photography technique to study the initial motion of particles leaving a ground surface. Similarly, Foucaut and Stanislas (1997) extracted 'dashed' particle lines from video images of saltating particles. They linked the particle lines to obtain the characteristic heights and lengths of the initial trajectories. Ryoichi et al. (2001) used a high-speed camera to measure the initial ejection velocities and rotational speeds of polypropylene particles (d = 500 μm and 1500 μm) over a rough bed consisting of particles of the same size. They traced the particle motion by releasing one particle at a time. Zou et al. (2001) investigated the variation of velocity and energy flux of saltating sand particles in a boundary layer using a high-speed multi-flash photography. Based on the experimental data, they established a statistical model for the velocity and energy distributions of sand particles.

When a cinematic photography or multiple-image photography method is applied, the constraints of the exposure time, the aperture of camera lens and strong ambient light scattering

make it difficult to record whole particle trajectories clearly. Especially, the initial and final stages of particle trajectories are often not clear on photographs. Therefore, the resulting entire trajectories reconstructed from the incomplete captured trajectories using an extrapolation scheme may contain some errors, depending on the criteria and the algorithm used.

Since the saltation of sand particles in air is a kind of stochastic process, the statistical analysis is essential for studying the dynamics of saltating particles. The statistical analysis was performed based on the particle trajectories, either captured directly or reconstructed indirectly with a series of consecutive images using digital image processing techniques (Nalpanis et al., 1993; Nishimura and Hunt, 2000; Machac and Rösgen, 2003). The conventional approach of detecting particle trajectories is basically dependent on identification of the same individual particle in a sequence. However, this is a time-consuming procedure, since hundreds of trajectory samples are required to get reliable statistical results.

The main objective of this study is to visualize the sand movement in a simulated atmospheric boundary layer (ABL) using a high-speed digital photography. The sand particle saltation in the region very close to the bed surface was observed with a high temporal and spatial resolution. In addition, the instantaneous particle velocity fields were obtained using a particle tracking velocimetry (PTV) method and then the trajectories of saltating particles were evaluated statistically.

2. Experimental Methods

2.1 Wind Tunnel

Experiments were performed in an open-type subsonic wind tunnel with a test section of 6.75 m^L × 0.72 m^W × 0.6 m^H. Spires of a height around 0.28 m and artificial grass with a fetch length of 0.5 m were installed at the entrance of the wind tunnel to simulate a neutral ABL.

The velocity profiles of oncoming wind were measured using an I-type hot-wire probe (DANTEC 55P11) connected to a constant-temperature hot-wire anemometer (TSI IFA-100). The mean streamwise velocity profiles measured at two free-stream velocities of 7 and 8 m/s are shown in Fig. 1. They are well fitted with the logarithmic law $U(y) = u_* / \kappa \cdot \log(y / y_0)$, where $U(y)$ is the mean streamwise velocity, u_* is the friction velocity, κ is von Karman constant, and y_0 is the effective roughness length. The streamwise turbulence intensity at ground surface was about 10 %.

The saltation layer generally extends to 0.05 – 0.10 m above the sand bed surface. In this study, thickness of the simulated ABL (δ) is about 0.25 m, ensuring that saltation occurs inside the lower part of the ABL surface layer. In addition, the trajectories of saltating particles usually can be reconstructed accurately in cases of relatively low particle concentration. We performed the experiments at the friction velocity (u_*) of 0.28 m/s, about 10 % higher than the threshold friction velocity (u_{*t}).

Natural sand with a density of 2650 kg/m^3 was collected from nearby local beach. Sand particles in the range of d = 200-300 μm were selected using standard sieves. The sand samples were dried in a constant temperature oven (105 °C) for 8 hours prior to wind tunnel experiments, to ensure that water contents in the sand samples are very low. The present study was focused on the movement of saltating dry sand particles and the effect of sand bed surface moisture and air humidity was neglected. The sand sample was spread evenly over the bottom surface of the wind tunnel test section, with a dimension of 1.0 m^L × 0.2 m^W × 0.01 m^H. A pair of aluminum bars with a height of 10 mm, were used as barriers to contain the sand sample. The sand bed was located at X = 5.5 m ($\geq 25\delta$) downstream from the entrance of the test section to establish an equilibrium state of saltation flow. Prior to each test, the sand bed surface was leveled carefully to be flush with the tops of the barrier bars.

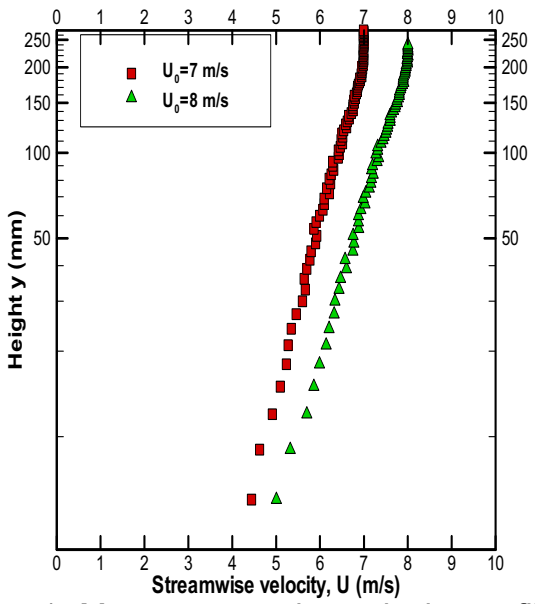

Fig. 1. Mean streamwise velocity profiles of the simulated atmospheric boundary layer.

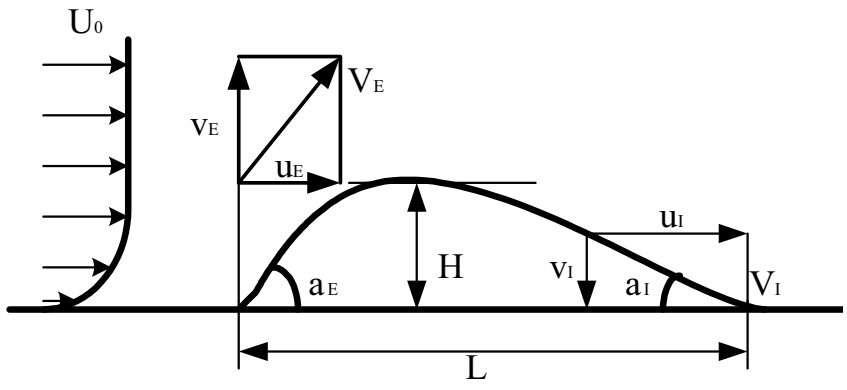

Fig. 2. Definition of physical quantities of saltating particle trajectories.

2.2 High-Speed Digital Photography

The vertical center plane of the test section was illuminated with a thin clod light sheet emitted from a halogen lamp. A high-speed CMOS camera (Photron FASTCAM-APX) was used to capture consecutive particle images with a spatial resolution of 1024 × 512 pixels at a frame rate of 2000 fps (frames per second). The exposure time for each frame was set to 1/3000 second to avoid streak patterns of high-speed particles. The FOV (field of view) was 136 mm × 78 mm (133 μm/pixel) for the side view and 136 mm × 136 mm for the plan view. To reduce strong light scattering from the aluminum barriers, they were covered with a black tape. For each run, 4096 frames were captured. Three runs were performed repeatedly under the same experimental condition.

2.3 Image Processing

The quality of raw particle images is usually degraded by light reflection from solid surfaces and by irregular scratches on the observation window. Most of these disturbances can be removed by subtracting a background image from individual particle images. The background image is obtained by averaging a large number of recordings. The adoption of this preprocessing procedure enabled us to observe the saltating particles more clearly than achieved in previous studies. Since the sand particle images were captured at 2000 fps with an exposure time of 1/3000 s, each image shows a "snap shot" of the saltating particles at a particular instant. The particles moving slowly appear as spots and high-speed particles appear as streaks. By overlapping a sequence of consecutive particle images, the trajectories of saltation particles can be reconstructed.

2.4 Statistical Analysis

We applied a PTV algorithm (Baek and Lee, 1996) to obtain the instantaneous velocity vector field of moving particles. The sand particles ejecting (lifting-off) or impacting within 1 mm above the sand bed surface were collected as statistical samples. The main physical quantities evaluated in this study are defined in Fig. 2, in which the subscripts 'E' and 'I' denote ejection and impact, respectively. Both the horizontal (u) and the vertical (v) velocity components were directly obtained from the instantaneous particle velocity data. The angle and resultant speed of ejection and impact were computed using the following formulas:

$$\alpha = \tan^{-1}(v/u),\ V = \sqrt{u^2 + v^2}$$

In order not to count the same particle repeatedly, particle velocity data from every 100 images were used. Compared with the conventional data processing methods, this approach can easily handle more particle samples for statistical analysis.

3. Results and Discussion

3.1 Saltation in the Windward Direction

From the reconstructed particle trajectories, various particle saltation modes were observed near the sand bed surface. Figure 3(a) shows a typical saltating particle trajectory. The wind blows from the left to the right side. And the bright horizontal line is the sand bed surface. The entire trajectory of a saltating particle, shown as a dashed curve, was obtained by overlapping every other particle images in a series. The oncoming wind makes the sand particle lift off the bed surface with an ejection angle of about 30°. This sand particle obtains additional momentum from the atmospheric wind flow, which increases its horizontal velocity component. After arriving at the maximum altitude, the sand particle starts to descend. During this descending motion, the vertical velocity component is also increased because of the gravity acting on it. Finally the sand particle impacts on the sand bed with a small impact angle (around 10°). It rebounds and starts another saltation process. This successive

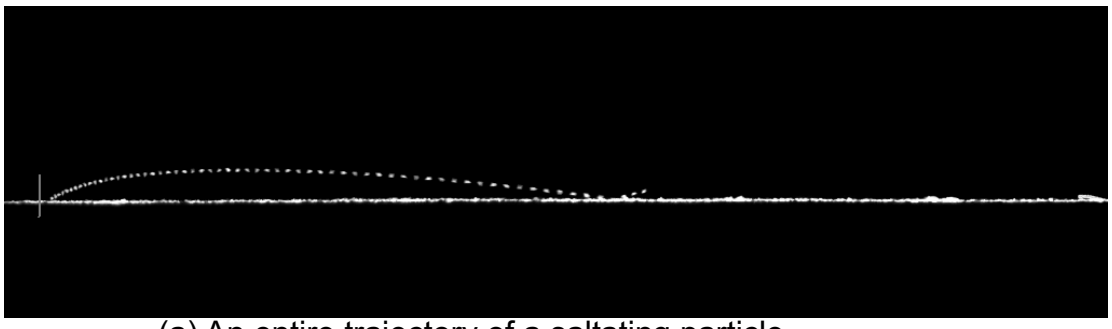

(a) An entire trajectory of a saltating particle

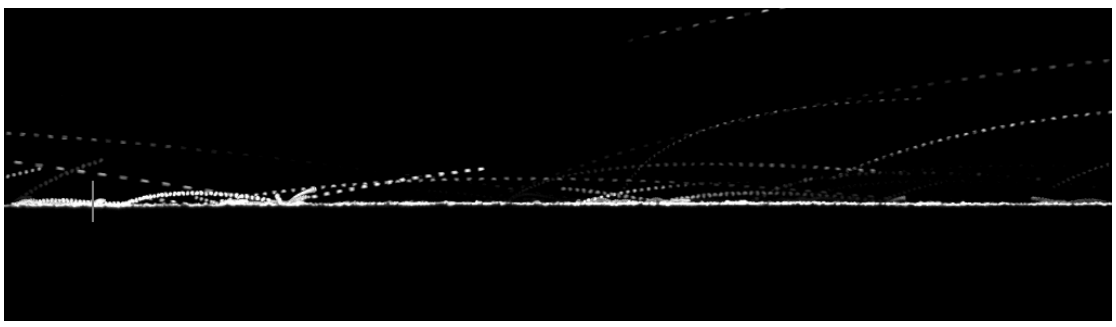

(b) A collision event involving one impactor and three ejectors

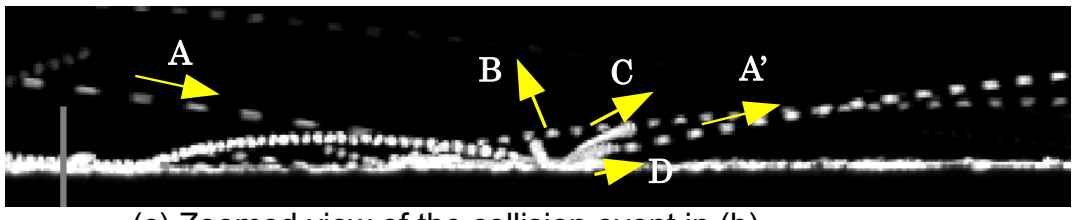

(c) Zoomed view of the collision event in (b)

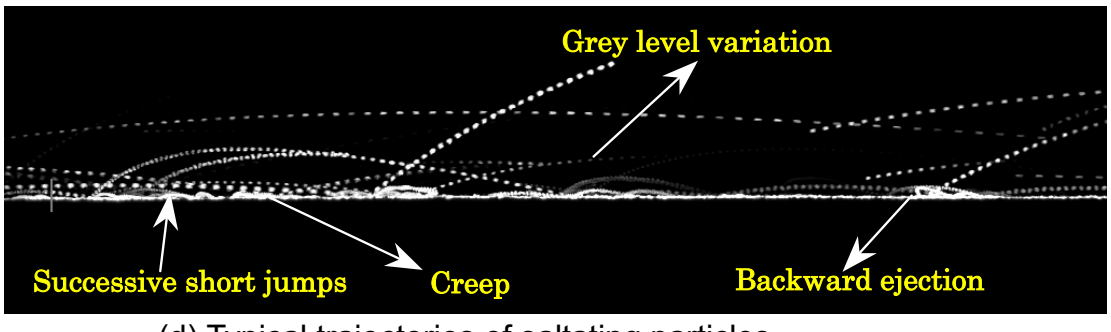

(d) Typical trajectories of saltating particles

Fig. 3. Various trajectories of saltating particles, with a FOV of 136 mm x 38 mm in (a), (b) and (d).

jump of sand particles represents a typical behavior of saltation. It can be easily found that, the particle speed in the descent segment is higher than that in the ascent segment, since the time

interval between two adjacent marks is constant (1/1000 s).

Figure 3(b) shows a typical collision event occurring between four particles. The close-up view of the collision event is clearly shown in Fig. 3(c). Particle A impacts on the sand bed surface, inducing a collision. The collision makes three stationary sand particles B, C and D lift off the surface. Particles C and D eject at a small angle less than 45°, while particle B ejects at an angle larger than 90°. Ejection is usually heading towards the windward direction either directly under wind force or indirectly by collision. Nevertheless, the backward ejection (opposite to the windward direction) is seldom observed and mostly occurs by collision. After colliding with particles B, C and D, particle A rebounds and continues its jumps. According to Willetts and Rice (1985), this collision can be mentioned to involve one "impactor" and three "ejectors". The number of ejectors could greatly vary from zero up to n (n = 4 ~ 10), depending on energy provided by the impactor and the accumulation mode of the particles on the sand bed surface. Besides, collision works as an important mechanism of inducing stationary particles to leap into air.

Figure 3(d) represents various trajectories of reconstructed saltating particles. In general, most particles can be assumed to have parabolic-shaped trajectories with a wide range of ejection angles, trajectory heights and lengths. Some short particle trajectories are visible just above the bed surface, the others show long displacements and considerable heights. The heights and lengths of particle trajectories are quite different case by case. Dong et al. (2002) also found that the ejection angle could be varied in a wide extent. This simple visualization confirms that the saltation of sand particles in air is a highly stochastic process and the statistical analysis is indispensable to understand the saltating particle trajectories.

Particle creep on the bed surface is also visible in Figs. 3(b) and (d). Some particles only roll over the surface, without leaping off it. The creep mode happens intermittently. However, in some cases, particles in creep motion are hard to discriminate clearly from particles saltating with a short displacement and a low height.

3.2 Transverse Motion

It is interesting to notice that the grey level varies slightly along trajectory of the same particle in Fig. 3(c). This may be attributed to the transverse motion of the saltating particles, which changes the distance between particles and the recording camera. To examine this possibility, a thin laser light sheet was positioned in a horizontal plane just above the flat sand bed surface and particle images were captured from top of the test section. In the raw image, the particles moving on the surface were clearly visualized. The image of particles moving away from the sand bed surface becomes blurry, because they are moving out of the laser light sheet. However, this does not influence significantly the reconstruction of the particle trajectories in the horizontal plane.

Several typical trajectories in the horizontal plane are shown in Fig. 4. Some trajectories appear as straight lines, while others show irregular-shaped curves. Two trajectories exhibit obvious turning points at marks A and B. This presumably results from a collision with another particle. Deviation of particle trajectories from the main streamwise direction occurs often on the sand bed surface, closely related to the impact and collision phenomena.

The observation indicates that saltating particles undergo relatively significant transverse motion. This deviation of particle trajectories seems to occur mainly due to impact and collision phenomena on the sand bed surface. Nino and Garcia (1998) mentioned that the transverse deviation of a particle in water was slightly larger than one particle diameter in a typical sand saltation and could be neglected. Sand particles in water are mainly transported in suspension, thus controlled by the turbulent characteristics of water flow. On the other hand, saltation is dominant for sand particle moving in air, especially in the region near the ground surface. Therefore, transport of sand particles in water and in air seems to have different mechanism. The present study shows that transverse motion of sand particles in air should be taken into account for accurate analysis.

The transport of sand particles in water and in air seems to have different mechanism. The most prominent feature of the sand movement in water is that sand particles are transported mainly

in suspension, thus controlled by the turbulent characteristics of water flow. On the other hand, saltation dominates the sand movement in air, especially near the ground surface.

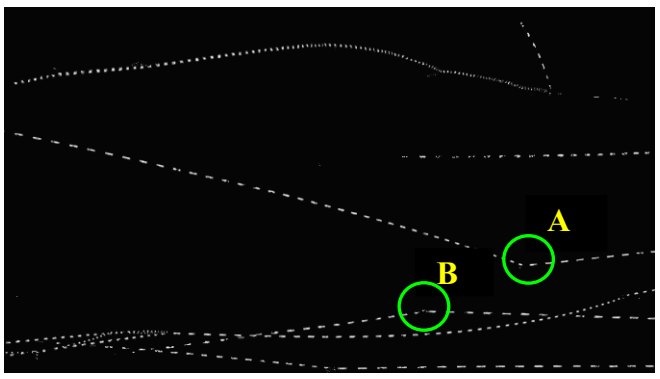

Fig. 4. Typical trajectories of saltating particles in transverse motion.

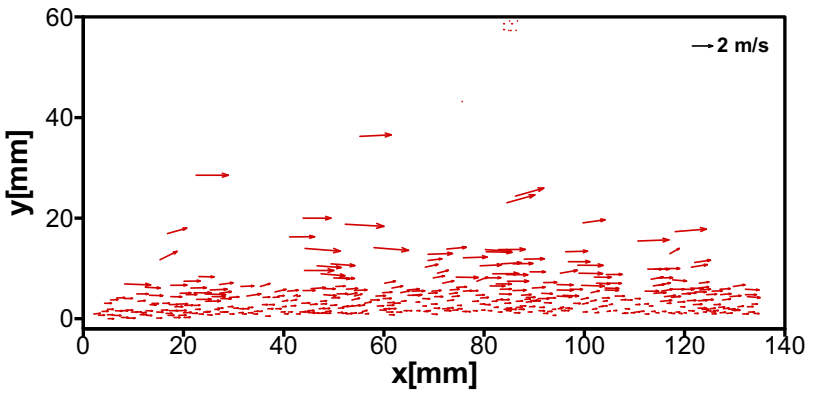

Fig. 5. Instantaneous velocity vector field of sand particles (d = 200 - 300 μm).

3.3 Statistics of Saltating Particle Trajectories

Figure 5 provides a typical instantaneous velocity field of sand particles, extracted with a PTV method. Most particles remain in the near surface region below y = 20 mm, only a few particles fly in higher altitude with a considerably high speed.

Based on the tracked velocity data of saltating particles, the probability density function (PDF) distributions of physical quantities related with ejection and impact events were statistically analyzed. Here the effect of sample number was also investigated. Figure 6 shows the PDF distributions of ejection velocities and ejection angle normalized by their mean values (denoted by <>) for three different sample amounts. The PDF distributions obtained from N = 400 and N = 600 agree quite well for all quantities inspected in this study. The results from N = 167 show similar trend, however their absolute magnitudes are somewhat different. Similarly, as shown in Fig. 7, the PDF distributions of impact particles estimated from N = 200 and N = 300 exhibit a better convergence than that from N = 77. This comparison indicates that 400 ejection samples and 200 impact samples are needed to get converged PDF distributions of related physical quantities.

The horizontal ejection velocity u_E ranges from 0 to 3.8 $\langle u_E \rangle$, where $\langle u_E \rangle$ denotes the time-averaged mean ejection velocity. The PDF distribution has a sharp peak around 38 % in the range of 0.8~1.2$\langle u_E \rangle$. The maximum PDF of the vertical ejection velocity occurs in the range of 0~0.4 $\langle v_E \rangle$ and its magnitude is gradually decreased with increasing $v_E/\langle v_E \rangle$. In addition, the percentage of particles lifting off the sand bed surface with high horizontal velocity ($u_E/\langle u_E \rangle$ = 1.6~3.6) and large vertical velocities ($v_E/\langle v_E \rangle$ = 2.0-3.2) is less than 10 %. This may result from energetic impacts of descending particles onto the surface. The PDF distribution of the ejection angle (α_E) does not differ greatly from that of the vertical ejection velocity, except that the range of large PDF values expands towards higher velocity range of $\alpha_E/\langle \alpha_E \rangle$ = 0~0.8. This tendency is understandable since the PDF distribution of the ejection angle reflects both of the horizontal and vertical ejection velocities.

Figure 7 shows the PDF distribution of the impact velocities and impact angles. The horizontal impact velocity shows a considerably sharp peak of about 48 % in the range of 0.8~1.2 $\langle u_I \rangle$. The vertical impact velocity (v_I) has the largest PDF value of 30 % in the ranges of 0~0.4 $\langle v_I \rangle$. The impact angle α_I exhibits a similar PDF distribution as that of the vertical velocity component.

All PDF distributions of the ejection and impact quantities show a clear mono-peak. This probably results from sufficient number of samples used in the statistical analysis. In addition, the PDF distribution of the horizontal velocity has a similar peak as that of Nalpanis et al. (1993). However, the PDF of the vertical velocity shifts towards the small-value range. The PDF distributions of the ejection and impact angles also move towards the small-value range. This seems to be attributed to that the sand particles even very close to the sand bed surface were included in this statistical analysis.

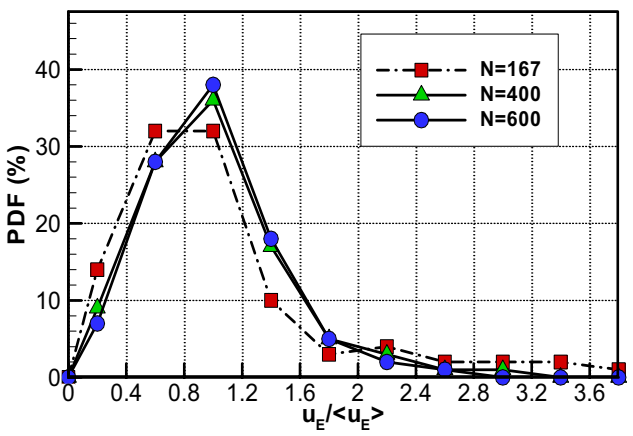

(a) Horizontal ejection velocity

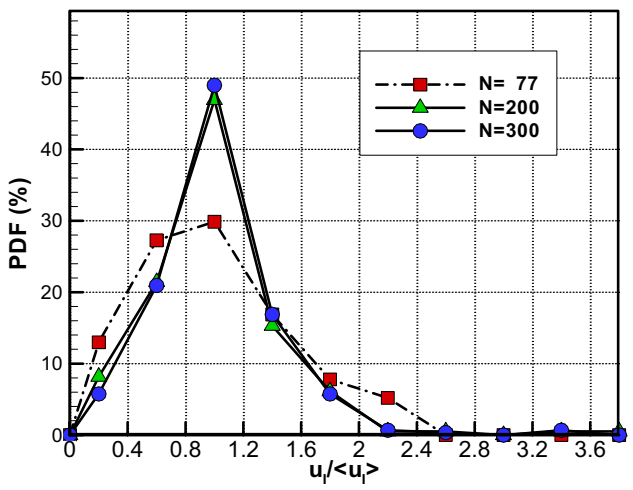

(a) Horizontal impact velocity

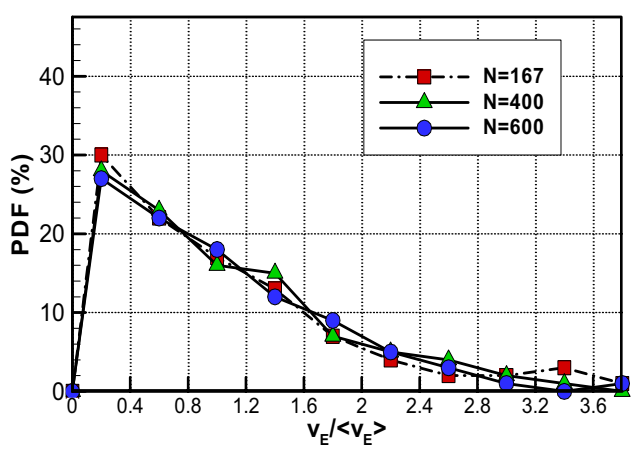

(b) Vertical ejection velocity

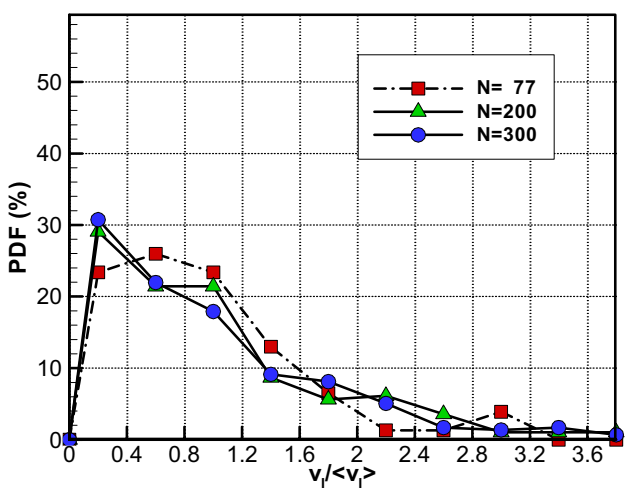

(b) Vertical impact velocity

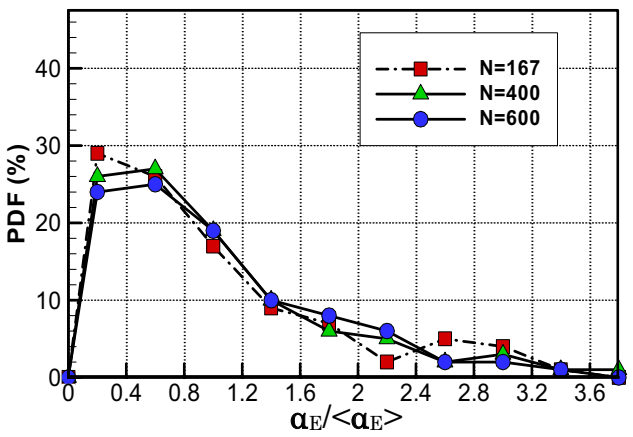

(c) Ejection angle

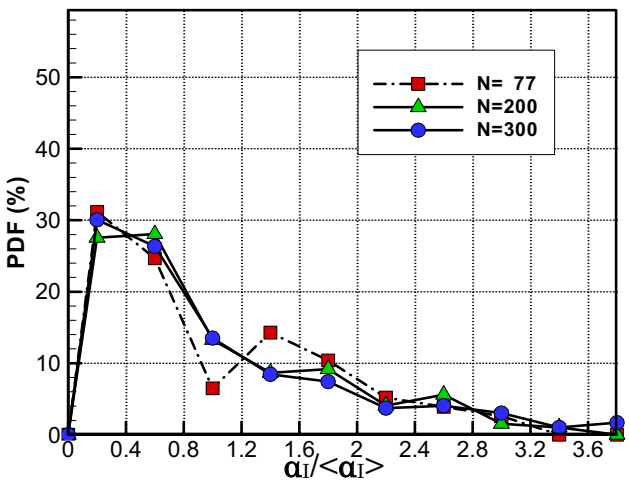

(c) Impact angle

Fig. 6. PDF distribution of ejection velocity and angle. Fig. 7. PDF distribution of impact velocity and angle.

4. Conclusion

The movement of natural sand particles in a simulated atmospheric boundary layer was visualized using a digital high-speed photography. Clear particle trajectories were reconstructed from the consecutive particle images captured at 2000 fps. Various saltation modes of sand particles were successfully observed in the region very close to the sand bed surface. The particle collision not only act as an important mechanism for inducing stationary particles to leap into air, but results in relatively large transverse motion of saltating sand particles.

The statistical analysis of the ejection and impact events of sand particles were conducted based on the instantaneous particle velocity field data obtained using a PTV method. 400 ejection

samples and 200 impact samples were used to get their PDF distributions. Peak locations of PDF distribution of the ejection and impact quantities are shifted towards the small-value range, due to inclusion of particles located close to the sand bed surface. These results would be helpful to understand the basic physics of sand saltation phenomena near the ground surface.

Acknowledgement

This work was supported by National Research Laboratory (NRL) Program of Ministry of Science and Technology (MOST) of Korea.

References

Baek, S. J. and Lee, S. J., A New Two-Frame Particle Tracking Algorithm Using Match Probability, Experiments in Fluids, 22-1 (1996), 23-32.

Bagnold, R. A., The Physics of Blown Sand and Desert Dunes, (1954), Dover publications, Inc. Mineola, New York.

Dong, Z. B., Liu, F. L., Wang, H. T. and Zhao, A.G., Impact–Entrainment Relationship in a Saltating Cloud, Earth Surface Processes and Landforms, 27 (2002), 641-658.

Foucaut, J.-M. and Stanislas, M., Experimental Study of Saltating Particle Trajectories, Experiments in Fluids, 22 (1997), 321-326.

Machac, M. and Rösgen, T., Fluid Flow Visualization by Three-dimensionally Reconstruction Tracer Path Lines, Journal of Visulaization, 6-2 (2003), 115-124.

Nalpanis, P., Hunt, J. C. R. and Barrett, C. F., Saltating Particles over Flat Beds, Journal of Fluid Mechanics, 251 (1993), 661-685.

Nino, Y. and Garcia, M., Experiments on Saltation of Sand in Water, Journal of Hydraulic Engineering, 124-10 (1998), 1014-1025.

Nishimura, K. and Hunt, J. C. R., Saltation and Incipient Suspension above a Flat Particle Bed below a Turbulent Boundary Layer, Journal of Fluid Mechanics, 417 (2000), 77-102.

Kurose, R., Makino, H. and Komori, S., Particle Trajectory in Turbulent Boundary Layer at High Particle Reynolds Number, Journal of Fluids Engineering, 123 (2001), 956-958.

Willetts, B.B. and Rice, M. A., Intersaltation Collisions, Proceedings of International Workshop on the Physics of Blown Sand, University of Aarhus (Denmark), 1 (1985), 83-100.

Zou, X. Y., Wang, Z. L., Hao, Q. Z., Zhang, C. L., Liu, Y. Z. and Dong, G. R., The Distribution of Velocity and Energy of Saltating Sand Grains in a Wind Tunnel, Geomorphology, 36-3-4 (2001), 155-165.

Author Profile

Wei Zhang: She received her M.Sc (Eng) in Heating, Ventilation and Air Conditioning from Xi'an University of Architecture and Technology in 1999. She received her Ph.D. in Fluid Engineering and Turbomachinery from Xi'an Jiaotong University in 2003. Then she worked as a postdoctoral researcher in Pohang University of Science and Technology (POSTECH) till Feb., 2006. Currently she is working at the Institute of Fluid Mechanics, Technical University of Braunschweig, Germany as a guest scholar. Her research interests are wind engineering, flow visualization, bluff-body aerodynamics, and flow control techniques.

Jong Hoon Kang: He received his master degree in Mechanical Engineering in 2004 from POSTECH. He is a Ph.D student at POSTECH and his research interests are PSP technique and wind engineering.

Sang Joon Lee: He received his MSc and Ph.D. in Mechanical Engineering from KAIST (Korea Advanced Institute of Science and Tech.) in 1982 and 1986, respectively. In 1986 he worked as a senior researcher at KIMM. He joined the Department of Mechanical Engineering at POSTECH as an Assistant Professor in 1987, and in 1999 he became a full professor. His research interests include quantitative flow visualization (PIV, PTV, LIF, and Holography), experimental fluid mechanics, bluff body aerodynamics, microfluidics, and flow control.